01

Energetic and radiative properties of the $A^2\Sigma^+ - X^2\Pi$ system of the OH radical: *ab initio* calculation and non-adiabatic simulation

© S.V. Kozlov, E.A. Pazyuk

Moscow State University,
119991 Moscow, Russia

e-mail: kozlovsv@my.msu.ru, pazyuk@phys.chem.msu.ru

Received August 11, 2022
Revised September 6, 2022
Accepted October 18, 2022

A quantum-chemical model for non-adiabatic simulation of the energetic and radiative properties of the $A^2\Sigma^+ - X^2\Pi$ system of the OH radical is presented. The electronic structure parameters (potential energy functions and electronic matrix elements of the spin-orbit and the electron-rotation interactions) are obtained by means of *ab initio* calculation. The reliability of the performed calculations is confirmed by comparing *ab initio* estimates with experimental values for the spin-orbit splitting, the Λ-doubling parameters of the $X^2\Pi$ state, and the γ-doubling of the $A^2\Sigma^+$ state. The frequencies and Einstein coefficients for rovibronic transitions between the $A^2\Sigma^+$ and $X^2\Pi$ states are simulated in a wide range of rovibrational excitations. The obtained values are in quantitative agreement with the data available from literature.

Keywords: OH radical, *ab initio* calculation, non-adiabatic interaction, fine structure, radiative transition probability.

DOI: 10.21883/EOS.2022.12.55236.4015-22

Introduction

The OH radical is widely known primarily due to numerous astronomical observations, being one of the first molecules unambiguously identified in the interstellar medium. It has been reliably detected in the spectra of stellar atmospheres [1], including the Sun [2], in interstellar clouds [3] and in the atmospheres of planets [4] . Radiative OH transitions serve as a probe for determining the oxygen content near the surface of stars. The OH radical is considered one of the main oxidizing agents in the Earth's atmosphere [5], capable of removing toxic organic compounds due to its high reactivity [6,7]. Vibrational-rotational transitions OH ($X^2\Pi$) are the source of the nightglow of the atmosphere and are known as the Meinel bands [8–10]. In addition to participating in purely astronomical and atmospheric processes, the OH radical is a key link in many high-temperature technological processes [11].

There is an extensive literature on OH spectroscopy. The electronic transition $A^2\Sigma^+ - X^2\Pi$ [12–22] has been studied in the most. The spectral database HITRAN [23], which is a compilation of experimental and calculated data, contains more than nine thousand frequencies of the corresponding rovibronic transitions. In addition, electronic transitions have been registered and analyzed. $B^2\Sigma^+ - X^2\Pi$ [14,24–27], $C^2\Sigma^+ - X^2\Pi$ [14], $a^2\Sigma^- - X^2\Pi$ [28] and $C'^2\Pi - X^2\Pi$ [29].

The main disadvantage of the currently available spectral information is the lack of a universal spectral model with good extrapolation capabilities, which would allow one to go beyond the current experimental data and to simulate transitions not yet observed at the required level of accuracy. The sets of molecular constants currently used to analyze the structure of the $A^2\Sigma^+ - X^2\Pi$ transition [17] were obtained in within the framework of the phenomenological method of the effective Hamiltonian for a limited range of vibrational-rotational excitation, which makes it difficult to predict the energy and radiation characteristics at large values of vibrational-rotational excitation, when it becomes necessary to go beyond the adiabatic approximation. This problem becomes especially topical when analyzing the processes of water photolysis, when rotationally highly excited OH radicals, the so-called superrotators [30], are formed.

An alternative method for analyzing high-resolution electronic spectra, based on the direct numerical solution of a system of nonadiabatic coupled radial Schrödinger equations, makes it possible to model the rovibronic structure taking into account both weak regular and strong local intramolecular perturbations, which significantly affect both energy and radiation characteristics — especially with increasing energy of vibrational-rotational excitation. The possibility of practical implementation of this method of coupled vibrational channels is determined primarily by the development of a rigorous quantum mechanical model of nonadiabatic description and the use of high-precision quantum chemistry methods for calculating the potential energy functions and the corresponding electronic matrix elements of spin-orbit and electron-rotational intramolecular interactions. The purpose of this work is to implement such a non-adiabatic approach for modeling the rovibron structure of the electronic transition $A^2\Sigma^+ - X^2\Pi$ the OH radical.

Non-adiabatic model

The values of energies and wave functions of nonadiabatic terms necessary for modeling the rovibron structure of the $A^2\Sigma^+ - X^2\Pi$ transition in the framework of the coupled channel method (coupled channels, CC) can be obtained by solving a system of three coupled radial equations:

$$\left[-\mathrm{I}\frac{\hbar^2}{2\mu}\frac{d^2}{dR^2} + \mathrm{V}(R) - \mathrm{I}E^{\mathrm{CC}}\right]\mathbf{\Phi} = 0, \quad (1)$$

where I-is the identity matrix 3×3, $\mathbf{\Phi}$ -is the column vector (3×1) containing the components of the vibronic wave function φ_i, V is potential energy matrix (3×3), which, taking into account spin-orbital and electron-rotational intramolecular interactions, is arranged as follows:

$$V^{e/f}_{X_{1/2}} = U_X - \frac{1}{2}\xi_X + BY^2, \quad (2)$$

$$V^{e/f}_{X_{3/2}} = U_X + \frac{1}{2}\xi_X + B[Y^2 - 2], \quad (3)$$

$$V^{e/f}_{A} = U_A + B[Y^2 \mp Y], \quad (4)$$

$$V^{e/f}_{X_{1/2}-X_{3/2}} = -B\sqrt{Y^2 - 1}, \quad (5)$$

$$V^{e/f}_{X_{1/2}-A} = \xi_{XA} + BL_{XA}[1 \mp Y], \quad (6)$$

$$V^{e/f}_{X_{3/2}-A} = -BL_{XA}\sqrt{Y^2 - 1}. \quad (7)$$

Here $Y \equiv J + 0.5$ (J is rotational quantum number), $B \equiv 1/2\mu R^2$ (μ is reduced mass), U_X and U_A are potential energy functions of states $X^2\Pi$ and $A^2\Sigma^+$, ξ_X is spin-orbit splitting function of state $X^2\Pi$, ξ_{XA} and L_{XA} are spin-orbit and electron-rotational interaction functions between the $X^2\Pi$ and $A^2\Sigma^+$ states. The sign of $\mp$ is determined by the parity: $-$, $+$ for e-, f-levels respectively. It should be emphasized that all the electronic parameters included in the potential energy matrix are explicit functions of the internuclear distance R and can be obtained in the framework of *ab initio* calculations.

The data in the HITRAN [23] database for transitions between the rovibronic levels of the states $X^2\Pi$ and $A^2\Sigma^+$ are limited by the ranges of rotational $J \in [0.5, 36.5]$ and vibrational $v'' \in [0.9]$, $v' \in [0.4]$ quantum numbers, which allows us to assume the regular nature of mutual perturbations caused by interactions between these states (Fig. 1). To simulate these transitions, the quantum chemical model can be simplified, and within the framework of a reduced version of the coupled channel method [31] intramolecular interactions can be estimated using Van Vleck contact transformations. Then the original matrix is reduced to a block-diagonal form. For the state $X^2\Pi$, the effective matrix has modified matrix elements:

$$\tilde{V}^{e/f}_{X_{1/2}} = V^{e/f}_{X_{1/2}} + V_S + 2V_{SL}[1 \mp Y] + V_L[1 \mp Y]^2, \quad (8)$$

$$\tilde{V}^{e/f}_{X_{3/2}} = V^{e/f}_{X_{3/2}} + V_L[Y^2 - 1], \quad (9)$$

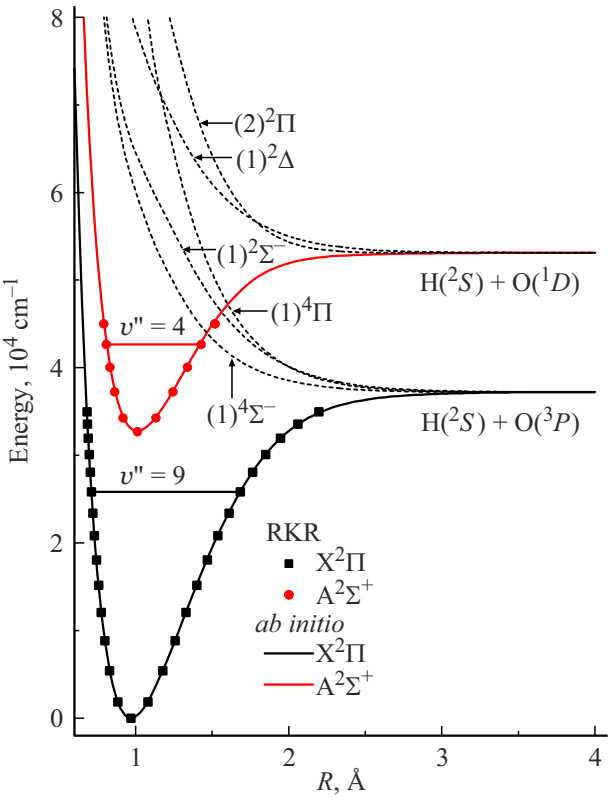

Figure 1. Potential energy functions of the electronic states of the OH radical converging to the first two dissociation limits. Solid and dashed curves are calculated *ab initio* functions, squares and circles -i.e. RKR potentials of states $X^2\Pi$ [10,33] and $A^2\Sigma^+$ [15].

$$\tilde{V}^{e/f}_{X_{1/2}-X_{3/2}} = V^{e/f}_{X_{1/2}-X_{3/2}} + (V_{SL} + V_L[1 \mp Y])\sqrt{Y^2 - 1}, \quad (10)$$

where the introduced second-order corrections are defined as

$$V_S(R) = \frac{\xi^2_{XA}}{U_X - U_A}, \quad (11)$$

$$V_{SL}(R) = B\frac{\xi_{XA}L_{XA}}{U_X - U_A}, \quad (12)$$

$$V_L(R) = B^2\frac{L^2_{XA}}{U_X - U_A}. \quad (13)$$

For the state $A^2\Sigma^+$, the effective potential has the form

$$\tilde{V}^{e/f}_{A} = V^{e/f}_{A} - V_S - 2V_{SL}[1 \mp Y] - V_L[1 \mp Y]^2. \quad (14)$$

The potential energy functions, electronic matrix elements of nonadiabatic interactions and the dipole moment of the electronic transition, necessary for the implementation of the proposed model, were obtained in the framework of *ab initio* calculations.

Ab initio calculations

All performed *ab initio* calculations were carried out in the MOLPRO 2010 [32] package. The aug-cc-pV5Z and aug-cc-pwCV5Z basis sets were used to describe the H

and O atoms, respectively. To take into account the static correlation, we used the method of multiconfigurational self-consistent field in the full active space with averaging over target states (SA-CASSCF) with the inclusion of 6, 2, 2 and 0 orbitals of symmetry A_1, B_1, B_2, and A_2 into the active space (including the oxygen core orbital). To account for dynamic correlation, the multiconfiguration reference configuration interaction (MRCI) method was used. When calculating the potential energy function for doublet and quartet states converging to the first two dissociation limits, all 7 states were included in the averaging (SA-CASSCF). The results are shown in Fig. 1. The main series of calculations was performed with optimization only for the target states $A^2\Sigma^+$ and $X^2\Pi$. All calculations were performed in the range of internuclear distances R from 0.6 to 8 Å with a step of 0.05–0.1 Å to $R = 5$ Å and with a step of 0.5 AA next.

The deviation of the calculated excitation energy $U_A(R) - U_X(R)$ from the analogous value obtained for the RKR potentials $X^2\Pi$ [10,33] and $A^2\Sigma^+$ [15], in the region of internuclear distances 0.8–1.5 Å lies in the range from 50 to 180 cm^{-1}, which corresponds to $\sim 0.5\%$ of the absolute value ($\sim 33\,000\,cm^{-1}$). At the dissociation limit, the difference between the calculated energies for the states $A^2\Sigma^+$ and $X^2\Pi$ was 15828 cm^{-1}. This value is close to the atomic transition energy $O(^3P)$–$O(^1D)$, which, taking into account the averaging over the spin of the components, $O(^3P)$ is 15789.887 cm^{-1} [34]. The calculated values of equilibrium internuclear distances for $X^2\Pi$ and $A^2\Sigma^+$ are 0.9699 and 1.0118 Å respectively. These values practically do not differ from the experimental data (0.9701 Å for $X^2\Pi$ [10] and 1.0114 Å for $A^2\Sigma^+$ [15]).

The electronic transition dipole moment functions $A^2\Sigma^+ - X^2\Pi$ and nonadiabatic matrix elements are calculated using the corresponding one-electron operators built into the package MOLPRO, and electronic wave functions obtained within the configuration interaction method. Fig, 2 shows the spin-orbit splitting functions ($\xi_X(R)$) of the $X^2\Pi$ state; spin-orbit ($\xi_{XA}(R)$) and electron-rotational ($L_{XA}(R)$) interactions and dipole moment electronic transition ($d_{XA}(R)$) between states $X^2\Pi$ and $A^2\Sigma^+$ Comparison with the data available in the literature [15,17,35] shows that there is good agreement between them.

The resulting matrix elements of the spin-orbit $\xi(R)$ and electron-rotation $L(R)$ interactions were used to estimate the fine structure parameters of the considered states [36]:
of spin-orbit splitting $X^2\Pi$

$$A(v'') = \langle \varphi^X_{v''} | \xi_X(R) - V_S(R) | \varphi^X_{v''} \rangle, \qquad (15)$$

of Λ-doubling parameters in $X^2\Pi$

$$q(v'') = 2\langle \varphi^X_{v''} | V_L(R) | \varphi^X_{v''} \rangle, \qquad (16)$$

$$p(v'') = 4\langle \varphi^X_{v''} | V_{SL}(R) | \varphi^X_{v''} \rangle, \qquad (17)$$

of γ-doubling parameter in $A^2\Sigma^+$

$$\gamma(v') = 4\langle \varphi^A_{v'} | V_{SL}(R) | \varphi^A_{v'} \rangle. \qquad (18)$$

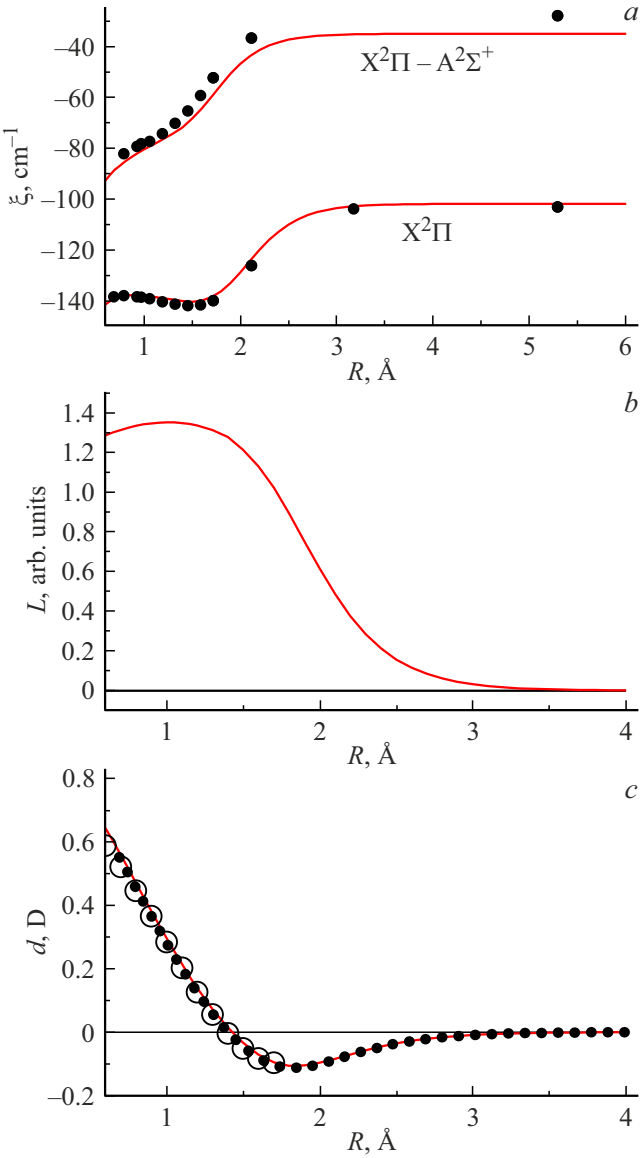

Figure 2. (*a*) Spin-orbit splitting for the $X^2\Pi$ state and spin-orbit interaction between the $X^2\Pi$ and $A^2\Sigma^+$ states: solid curves (data obtained in this work) and black circles (values calculated in the paper [35]) (*b*) Electron-rotational interaction between the $X^2\Pi$ and $A^2\Sigma^+$ states. (*c*) Dipole moment of the electronic transition $X^2\Pi$–$A^2\Sigma^+$: solid curves is the data obtained in this work, black circles are values calculated in the work [17], light circles is empirical function [15].

Here V_S, V_L and V_{SL} — are the above corrections for perturbation theory (11), (12) and (13). The vibrational wave functions of the levels $\varphi^X_{v''}$ and $\varphi^A_{v'}$ were found by solving one-dimensional radial Schrödinger equations with potential energy functions U_X and U_A.

Fig. 3 shows the dependences of the obtained quantities $A(v'')$, $q(v'')$ and $p(v'')$ on the vibrational quantum number and their empirical analogs obtained by processing the experimental data within the effective Hamiltonian model [10]. The spin-orbit splitting $A(v'')$ coincides with the empirical

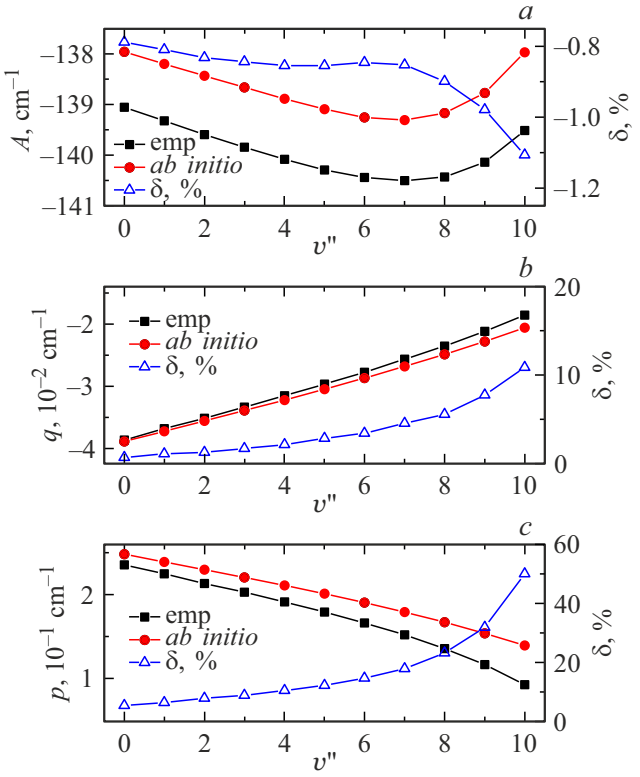

Figure 3. Calculated (*ab initio*) and empirical (emp) [10] spin-orbit splitting $A(v'')$ (*a*) and parameters Λ-doublings $q(v'')$ (*b*) and $p(v'')$ (*c*) for state $X^2\Pi$. Squares and circles are absolute values, triangles are relative errors.

Table 1. Calculated and empirical [17] values of the γ-doubling parameters (cm^{-1}) for the lowest vibrational levels v' of the $A^2\Sigma^s tate+$

v'	γ^{emp}	γ^{calc}	δ, %
0	0.2261	0.2281	0.9
1	0.2169	0.2174	0.2
2	0.2130	0.2064	−3.1
3	0.1960	0.1946	−0.7
4	0.1864	0.1813	−2.7

data for all vibrational levels. The deviation of the calculated values from the empirical ones practically does not depend on v'' and does not exceed 0.9% up to the level of $v'' = 8$, and for $v'' = 10$, 11 it is 0.9−1.1 %.

The parameter $q(v'')$ is described with an error of 1−5% for levels $v'' = 0$−6, then the deviation monotonically increases with growth v'' and for $v'' = 10$ reaches 12%. The parameter $p(v'')$ is described somewhat worse. And for $v'' = 0$−6 the error is 5−15%, but then it sharply increases and reaches 50% for $v'' = 10$.

Table 1 shows the calculated and empirical [17] values of the $\gamma(v')$-doubling parameters for the $A^2\Sigma^+$ state. The error in the description of this parameter increases almost monotonically from 1 to 3% as v' grows.

Ab initio estimates of the fine structure parameters confirm the reliability of the results of the calculations of potential energy functions and intramolecular interactions, as well as the adequacy of the proposed nonadiabatic model. An increase in the discrepancy with empirical data observed with an increase in the vibrational quantum number makes it possible to judge the range of excitation energies for which the perturbation theory is valid.

Simulation of rovibronic spectra

Taking into account the spin-orbit splitting in the $X^2\Pi_\Omega$ state, the splitting between the rotational *e*- and *f*-parity levels, and the selection rules for the rotational quantum number ($\Delta J = J' - J'' = 0, \pm 1$) in each $v'' - v''$ vibrational band of the $A^2\Sigma^+(v', J')$ transition $\rightarrow X^2\Pi(v'', J'')$ there are 12 rotational branches.

Q-branch ($J' - J'' = 0$):

Q_1 — transition $A^2\Sigma^+(e) \rightarrow X^2\Pi_{3/2}(f)$,

Q_{12} — transition $A^2\Sigma^+(e) \rightarrow X^2\Pi_{1/2}(f)$,

Q_2 — transition $A^2\Sigma^+(f) \rightarrow X^2\Pi_{1/2}(e)$,

Q_{21} — transition $A^2\Sigma^+(f) \rightarrow X^2\Pi_{3/2}(e)$.

P-branch ($J' - J'' = -1$):

P_1 — transition $A^2\Sigma^+(e) \rightarrow X^2\Pi_{3/2}(e)$,

P_{12} — transition $A^2\Sigma^+(e) \rightarrow X^2\Pi_{1/2}(e)$,

P_2 — transition $A^2\Sigma^+(f) \rightarrow X^2\Pi_{1/2}(f)$,

P_{21} — transition $A^2\Sigma^+(f) \rightarrow X^2\Pi_{3/2}(f)$.

R-branch ($J' - J'' = 1$):

R_1 — transition $A^2\Sigma^+(e) \rightarrow X^2\Pi_{3/2}(e)$,

R_{12} — transition $A^2\Sigma^+(e) \rightarrow X^2\Pi_{1/2}(e)$,

R_2 — transition $A^2\Sigma^+(f) \rightarrow X^2\Pi_{1/2}(f)$,

R_{21} — transitions$A^2\Sigma^+(f) \rightarrow X^2\Pi_{3/2}(f)$.

The assignment of transitions to the components $X^2\Pi_{1/2}$ and $X^2\Pi_{3/2}$ is conditional i.e. by the diagonal element in the potential energy matrix

Using the obtained *ab initio* potential energy functions and matrix elements of nonadiabatic interaction, within the framework of the proposed model, we calculated the frequencies of all possible transitions $A^2\Sigma^+(v', J') \rightarrow X^2\Pi(v'', J'')$ for the experimentally studied range of vibrational-rotational excitation. As a result, it was found that the *ab initio* frequencies of rovibronic transitions ($\nu = E(v', J') - E(v'', J'')$) differ by 50 −150 cm^{-1} from the experimental analogs for all the studied transitions, which agrees with the previously obtained error in estimating the excitation energy $X^2\Pi - A^2\Sigma^+$. As an illustration, Fig. 4 shows the frequency deviations ($\Delta\nu = \nu^{calc} - \nu^{exp}$) for the Q_1-branch depending on the rotational quantum number $J' = J'' \equiv J$ and vibrational quantum numbers in the ground (v'') and excited (v') electronic states. Fig. 4, *a* shows the dependence of the frequency deviation of the Q_1-branch for the band $v' = 0 \rightarrow v'' = 0$ on the rotational quantum number J . As can be seen, the absolute and relative errors increase monotonically with J, but the dependence is very weak (the relative error even at $J = 35$

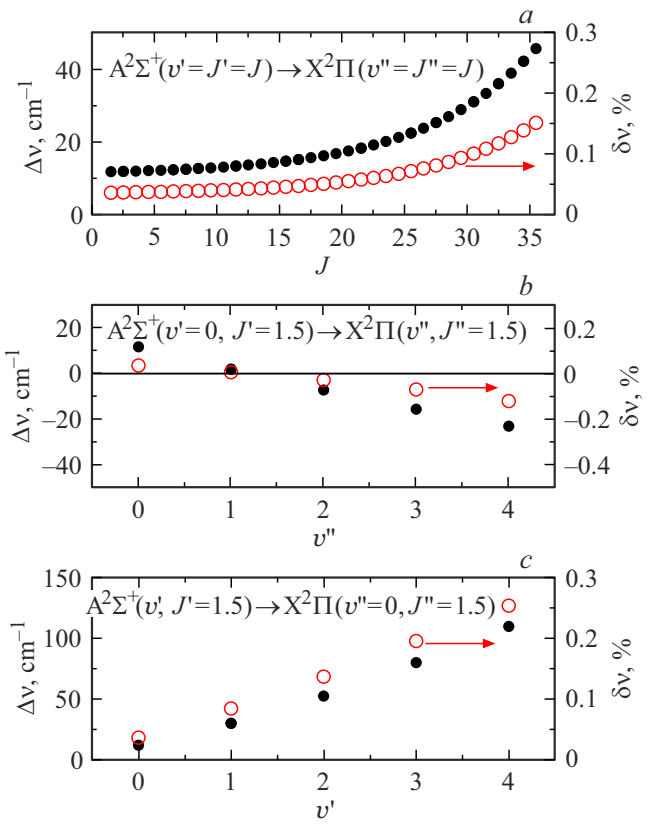

Figure 4. Absolute (black circles) and relative (red circles) deviations of the calculated transition frequencies of the Q_1 branch from the experimental values: *a* — $A^2\Sigma^+(v'=0, J) \rightarrow X^2\Pi(v''=0, J)$ depending on the rotational quantum number J; *b* is $A^2\Sigma^+(v'=0, J=1.5) \rightarrow X^2\Pi(v'', J=1.5)$ depending on vibrational quantum number v''; *c* is $A^2\Sigma^+(v', J=1.5) \rightarrow X^2\Pi(v''=0, J=1.5)$ depending on the vibrational quantum number v'.

;

is only 0.15%). The next panel (Fig. 4, *b*) shows the dependence of the frequency deviation of the Q_1-branch on the vibrational quantum number v'' for fixed values of $v'=0$ and $J=1.5$. For these transitions, the absolute value of the frequency decreases with increasing v'', passing through a minimum at $v''=1$, while the relative error remains in the range 0.2%. Dependence of the frequency deviation of the Q_1-branch on the vibrational quantum number v' for fixed values $v''=0$ and $J=1.5$ (Fig. 4, *c*) shows an increase in the absolute error with an increase in v', since the absolute value of the frequency increases for these transitions. The relative error also increases from 0.05 to 0.3%. For other branches and bands, a similar dependence of the errors in the calculation of the frequencies of rovibronic transitions on the value of the vibrational-rotational excitation is observed. These results indicate that the calculated functions included in the potential energy matrix have a correct radial dependence, and the proposed model correctly takes into account intramolecular interactions. This also makes it possible to count on a correct description of the nodal structure of the calculated vibrational-rotational wave functions both in the ground and in the excited electronic states, which determines to a large extent the probabilities of the corresponding transitions.

To estimate the probabilities of rovibronic transitions, one can use the corresponding Einstein coefficients for spontaneous emission $A^2\Sigma^+(v', J') \rightarrow X^2\Pi(v'', J'')$, which can be calculated as

$$A_{v'J'v''J''} = \frac{8\pi^2}{3\hbar\epsilon_0}\nu^3 M^2. \qquad (19)$$

Here ν is transition frequency, M is matrix element of transition dipole moment [37]:

$$M = M_{1/2}\begin{pmatrix} J'' & 1 & J' \\ -1/2 & 1 & -1/2 \end{pmatrix} \pm M_{3/2}\begin{pmatrix} J'' & 1 & J' \\ -3/2 & 1 & -1/2 \end{pmatrix}, \qquad (20)$$

$M_{1/2}$ and $M_{3/2}$ re integrals of the form

$$M_\Omega = \langle \varphi^A_{v'J'} | d_{XA}(R) | \varphi^{X_\Omega}_{v''J''} \rangle, \qquad (21)$$

where d_{XA} is the dipole moment function of the electronic transition $X^2\Pi \rightarrow A^2\Sigma^+$ (Fig. 2, *c*), $\varphi^{X_\Omega}_{v''J''}$ are components

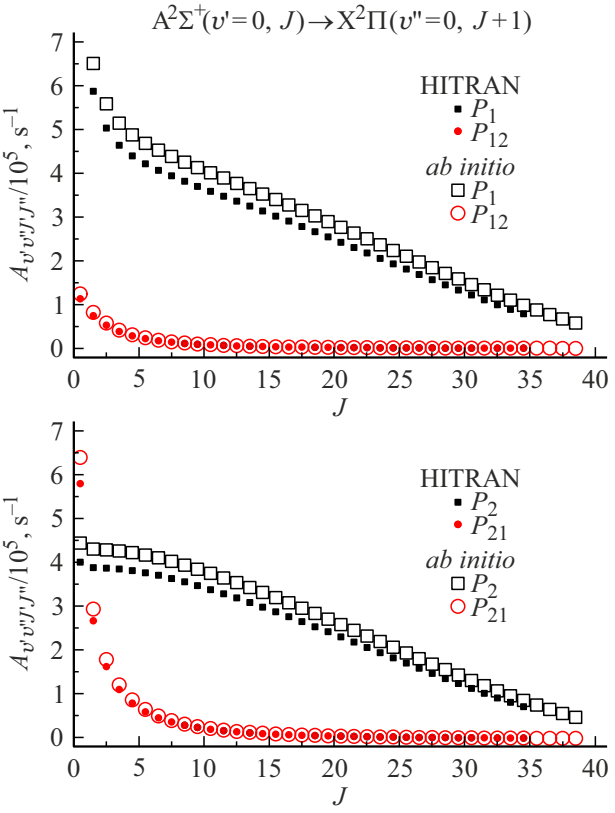

Figure 5. Dependence of the Einstein coefficients of the transitions $A^2\Sigma^+ \rightarrow X^2\Pi$ for P_1-, P_2-, P_{12}- and P_{21}-branches of the band $v'=0 \rightarrow v''=0$ of the rotational quantum number J ($J'=J$, $J''=J+1$).

of the wave function for rovibronic levels of states $X^2\Pi_\Omega$ obtained by solving the system of equations (1) with the matrix given by expressions (8)–(10), $\varphi^A_{v'J'}$ is wave function of rovibronic levels of the state $A^2\Sigma^+$ obtained by solving a one-dimensional radial equation with potential (14). The sign in expression (20) is determined by the branch type: „–“ for main branches (with indices 1 and 2) and „+“ for satellite branches (with indices 12 and 21).

According to these expressions, the Einstein coefficients $A_{v'J'v''J''}$ were calculated for all transitions in the experimentally studied range of vibrational and rotational quantum numbers. As illustrations, Figs 5–7 show the J-dependences of the calculated Einstein coefficients for the main and satellite branches of the band $v' = 0 \to v'' = 0$ and their analogues from the HITRAN base [23]. For all values of the rotational quantum number, there is a systematic overestimation of the *ab initio* coefficients $A_{v'J'v''J''}$ relative to the data [23] by 10–12%. This, apparently, is caused by the calculated function of the dipole moment of the electronic transition overestimated by 5–6% (Fig. 2, *c*), since the non-empirical frequency values for these transitions differ from the experimental ones by no more than 0.2% (Fig. 4, *a*). However, it should be noted that the deviation practically does not depend on either the type of branch or the value of rotational excitation.

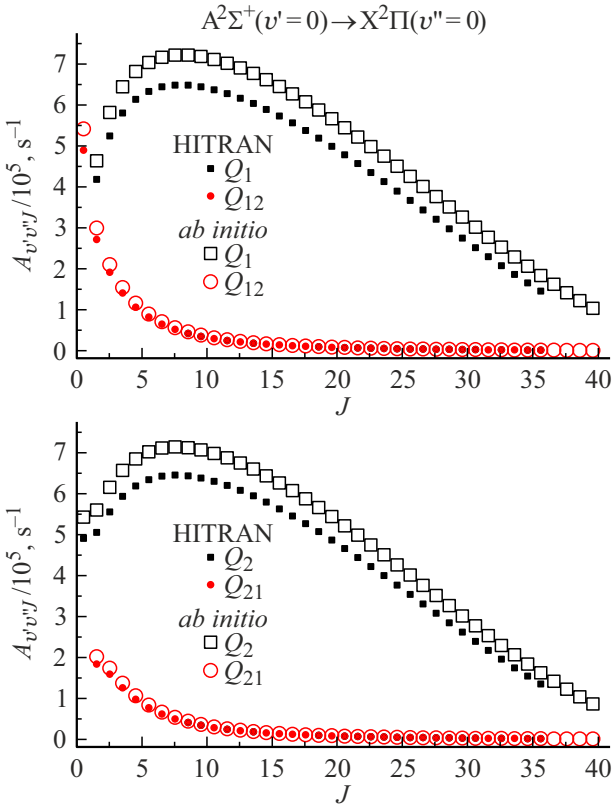

Figure 6. Dependence of the Einstein coefficients of the transitions $A^2\Sigma^+ - X^2\Pi$ for Q_1-, Q_2-, Q_{12}- and Q_{21}-branches of the band $v' = 0 \to v'' = 0$ of the rotational quantum number J ($J' = J'' = J$).

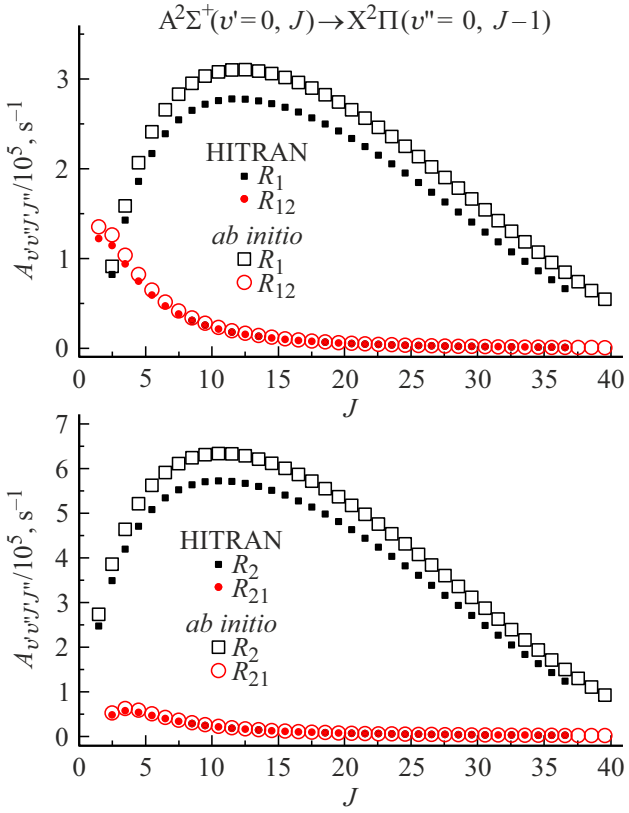

Figure 7. Dependence of the Einstein coefficients of the transitions $A^2\Sigma^+ - X^2\Pi$ for R_1-, R_2-, R_{12}- and R_{21}-branches of the band $v' = 0 \to v'' = 0$ of the rotational quantum number J ($J' = J$, $J'' = J - 1$).

The system $A^2\Sigma^+ - X^2\Pi$ is practically diagonal, and with increasing vibrational excitation the Einstein coefficients $A_{v'J'v''J''}$ in progressions decrease sharply. The range of their change is 6–7 orders. Table 2 gives the Einstein coefficients $A_{v'J'v''J''}$ for the Q_1-branch at a fixed value $J' = J'' = 1.5$, calculated within the framework of the proposed model for the vibrational bands registered in the work [15]. To estimate the effect of the transition dipole moment function $A^2\Sigma^+ - X^2\Pi$, the same quantities were calculated with the function found from the experimental data [15]. Comparison of both versions of the calculation with the HITRAN [23] database data indicates that in this case the discrepancy between the *ab initio* and experimental frequencies of rovibronic transitions makes a significant contribution to the error of the Einstein coefficients A^{ab}, which agrees with previous estimates (Fig. 4, *b, c*). Despite rather large errors in the absolute values of A^{ab}, the Einstein coefficients, calculated only on the basis of non-empirical data, absolutely correctly reproduce the sharp drop in literary analogues [23] with an increase in v'' in each progression in v', which also confirms the adequacy of the proposed model.

Table 2. The Einstein coefficients $A_{v'v''}$ (s^{-1}) for the Q_1-branch at $J' = J'' = 1.5$ calculated by the equation (19) with non-empirical function d_{XA} (Fig. 2, *c*) (A^{ab}) and with empirical function of transition dipole moment [15] (A^{emp}); HITRAN is data from the HITRAN database [23]

$v' - v''$	A^{ab}	A^{emp}	HITRAN
0–0	$4.627 \cdot 10^5$	$4.222 \cdot 10^5$	$4.173 \cdot 10^5$
0–1	$3.012 \cdot 10^3$	$2.424 \cdot 10^3$	$1.743 \cdot 10^3$
0–2	28.73	66.50	34.92
0–3	2.109	2.946	2.623
0–4	$1.071 \cdot 10^{-2}$	$1.148 \cdot 10^{-2}$	$1.141 \cdot 10^{-2}$
1–0	$1.492 \cdot 10^5$	$1.388 \cdot 10^5$	$1.355 \cdot 10^5$
1–1	$2.770 \cdot 10^5$	$2.474 \cdot 10^5$	$2.488 \cdot 10^5$
1–2	$3.996 \cdot 10^3$	$2.850 \cdot 10^3$	$2.145 \cdot 10^3$
1–3	$1.304 \cdot 10^2$	$2.760 \cdot 10^2$	$1.629 \cdot 10^2$
1–4	12.46	16.99	15.70
1–5	$9.330 \cdot 10^{-2}$	$8.452 \cdot 10^{-2}$	$9.793 \cdot 10^{-2}$
2–0	$3.124 \cdot 10^4$	$2.843 \cdot 10^4$	$2.778 \cdot 10^4$
2–1	$2.176 \cdot 10^5$	$2.018 \cdot 10^5$	$1.984 \cdot 10^5$
2–2	$1.473 \cdot 10^5$	$1.277 \cdot 10^5$	$1.310 \cdot 10^5$
2–3	$3.417 \cdot 10^3$	$2.008 \cdot 10^3$	$1.565 \cdot 10^3$
2–4	$3.817 \cdot 10^2$	$7.420 \cdot 10^2$	$4.803 \cdot 10^2$
2–5	45.39	59.98	58.41
3–0	$5.929 \cdot 10^3$	$5.166 \cdot 10^3$	$5.101 \cdot 10^3$
3–1	$7.779 \cdot 10^4$	$7.151 \cdot 10^4$	$7.041 \cdot 10^4$
3–2	$2.196 \cdot 10^5$	$2.020 \cdot 10^5$	$1.998 \cdot 10^5$
3–3	$6.605 \cdot 10^4$	$5.498 \cdot 10^4$	$5.768 \cdot 10^4$
3–4	$2.048 \cdot 10^3$	$8.248 \cdot 10^2$	$6.486 \cdot 10^2$
3–5	$8.919 \cdot 10^2$	$1.600 \cdot 10^3$	$1.131 \cdot 10^3$
3–6	$1.321 \cdot 10^2$	$1.669 \cdot 10^2$	$1.738 \cdot 10^2$
4–0	$1.154 \cdot 10^3$	$9.511 \cdot 10^2$	$9.538 \cdot 10^2$
4–1	$2.186 \cdot 10^4$	$1.947 \cdot 10^4$	$1.942 \cdot 10^4$
4–2	$1.204 \cdot 10^5$	$1.114 \cdot 10^5$	$1.104 \cdot 10^5$
4–3	$1.759 \cdot 10^5$	$1.592 \cdot 10^5$	$1.586 \cdot 10^5$
4–4	$2.246 \cdot 10^4$	$1.773 \cdot 10^4$	$1.927 \cdot 10^4$
4–5	$7.343 \cdot 10^2$	88.08	55.94
4–6	$1.795 \cdot 10^3$	$2.955 \cdot 10^3$	$2.276 \cdot 10^3$
4–7	$3.487 \cdot 10^2$	$4.076 \cdot 10^2$	$4.503 \cdot 10^2$

Conclusion

A non-adiabatic model for describing the energy and radiation parameters of the $A^2\Sigma^+ - X^2\Pi$ system of the OH radical based on non-empirical calculations of the electronic structure is proposed. The numerical experiments performed have shown that the accuracy of the obtained *ab initio* estimates of the potential energy curves and nonadiabatic electronic matrix elements is sufficient for unambiguous vibrational assignment of the available experimental terms. The use of the analytical dependence of the matrix elements of the transition dipole moment on the rotational quantum number makes it easy to estimate the intensities of rovibronic transitions for high values of J, which is extremely important in identifying new lines recorded in high-temperature spectra. Further refinement of the structural parameters to the experimental level of accuracy is planned to be carried out within the framework of solving the inverse spectroscopic problem using the iterative method of solving the coupled radial Schrödinger equations using the precision spectral data on the energy of the rovibronic terms of the considered states available in the literature.

Funding

This study was supported by a grant from the Russian Science Foundation № 22-23-00272, https://rscf.ru/project/22-23-00272/

Conflict of interest

The authors declare that they have no conflict of interest.

References

[1] J. Meléndez, B. Barbuy. Astrophys. J., **575** (1), 474 (2002). DOI: 10.1086/341142
[2] M. Asplund, N. Grevesse, A.J. Sauval, C.A. Prieto, D. Kiselman. Astronomy & Astrophysics, **417** (2), 751 (2004). DOI: 10.1051/0004-6361:20034328
[3] J.R. Goicoechea, J. Cernicharo. Astrophys. J., **576** (1), 77 (2002). DOI: 10.1086/343062
[4] G. Piccioni, P. Drossart, L. Zasova, A. Migliorini, J.C. Gérard, F.P. Mills, A. Shakun, A. García Muñoz, N. Ignatiev, D. Grassi, V. Cottini, F.W. Taylor, S. Erard, Astronomy & Astrophysics, **483** (3), 29 (2008). DOI: 10.1051/0004-6361:200809761
[5] R.G. Prinn, R.F. Weiss, B.R. Miller, J. Huang, F.N. Alyea, D.M. Cunnold, P.J. Fraser, D.E. Hartleyand, P.G. Simmonds. Science, **269** (5221), 187 (1995). DOI: 10.1126/science.269.5221.187
[6] R. Atkinson, J. Arey. Chem. Rev., **103** (12), 4605 (2003). DOI: 10.1021/cr0206420
[7] J. Lelieveld, F.J. Dentener, W. Peters, M.C. Krol. Atmos. Chem. Phys., **4** (9/10), 2337 (2004). DOI: 10.5194/acp-4-2337-2004
[8] A.B. Meinel. Astrophys. J., **111**, 555 (1950). DOI: 10.1086/145321
[9] P.C. Cosby, T.G. Slanger. Can. J. Phys., **85** (2), 77 (2007). DOI: 10.1139/p06-088
[10] J.S. Brooke, P.F. Bernath, C.M. Western, C. Sneden, M. Afşar, G. Li, I.E. Gordon. JQSRT, **168**, 142 (2016). DOI: 10.1016/j.jqsrt.2015.07.021
[11] T.B. Settersten, R.L. Farrow, J.A. Gray. Chem. Phys. Lett., **369** (5–6), 584 (2003). DOI: 10.1016/S0009-2614(03)00022-8
[12] C. Amiot, J.P. Maillard, J. Chauville. J. Mol. Spectrosc., **87** (1), 196 (1981). DOI: 10.1016/0022-2852(81)90089-8
[13] J.A. Coxon. J. Mol. Spectrosc., **58** (1), 1 (1975). DOI: 10.1016/0022-2852(75)90153-8
[14] J.A. Coxon, A.D. Sappey, R.A. Copeland. J. Mol. Spectrosc., **145** (1), 41 (1991). DOI: 10.1016/0022-2852(91)90349-F
[15] J. Luque, D.R. Crosley. J. Chem. Phys., **109** (2), 439 (1998). DOI: 10.1063/1.476582
[16] K.L. Steffens, J. Luque, J.B. Jeffries, D.R. Crosley. J. Chem. Phys., **106** (15), 6262 (1997). DOI: 10.1063/1.473644

[17] M. Yousefi, P.F. Bernath, J. Hodges, T. Masseron. JQSRT, **217**, 416 (2018). DOI: 10.1016/j.jqsrt.2018.06.016
[18] J.A. Coxon. Can. J. Phys., **58** (7), 933–949 (1980). DOI: 10.1139/p80-129
[19] G. Stark, J.W. Brault, M.C. Abrams. JOSA B, **11** (1), 3-32 (1994) DOI: 10.1364/JOSAB.11.00000
[20] R.A. Copeland, J.B. Jeffries, D.R. Crosley. J. Mol. Spectrosc., **143** (1), 183–185 (1990). DOI: 10.1016/0022-2852(90)90270-Z
[21] E.L. Derro, I.B. Pollack, L.P. Dempsey, M.E. Greenslade, Yu. Lei, D.C. Radenovic, M.I. Lester. J. Chem. Phys., **122** (24), 244313 (2005). DOI: 10.1063/1.1937387
[22] O.N. Sulakshina, Yu.G. Borkov. Proc. SPIE, **11916**, 119160C (2021). DOI: 10.1117/12.2604362
[23] I.E. Gordon, L.S. Rothman, R.J. Hargreaves, R. Hashemi, E.V. Karlovets, F.M. Skinner, E.K. Conway, C. Hill, R.V. Kochanov, Y. Tan, P. Wcislo, A.A. Finenko, K. Nelson, P.F. Bernath, M. Birk, V. Boudon, A. Campargue, K.V. Chance, A. Coustenis, B.J. Drouin, J.-M. Flaud, R.R. Gamache, J.T. Hodges, D. Jacquemart, E.J. Mlawer, A.V. Nikitin, V.I. Perevalov, M. Rotger, J. Tennyson, G.C. Toon, H. Tran, V.G. Tyuterev, E.M. Adkins, A. Baker, A. Barbe, E. Cane, A.G. Csaszar, A. Dudaryonok, O. Egorov, A.J. Fleisher, H. Fleurbaey, A. Foltynowicz, T. Furtenbacher, J.J. Harrison, J.-M. Hartmann, V.-M. Horneman, X. Huang, T. Karman, J. Karns, S. Kassi, I. Kleiner, V. Kofman, F. Kwabia-Tchana, N.N. Lavrentieva, T.J. Lee, D.A. Long, A.A. Lukashevskaya, O.M. Lyulin, V.Yu. Makhnev, W. Matt, S.T. Massie, M. Melosso, S.N. Mikhailenko, D. Mondelain, H.S.P. Muller, O.V. Naumenko, A. Perrin, O.L. Polyansky, E. Raddaoui, P.L. Raston, Z.D. Reed, M. Rey, C. Richard, R. Tobi'as, I. Sadiek, D.W. Schwenke, E. Starikova, K. Sung, F. Tamassia, S.A. Tashkun, J. Vander Auwera, I.A. Vasilenko, A.A. Vigasin, G.L. Villanueva, B. Vispoel, G. Wagner, A. Yachmenev, S.N. Yurchenko. JQSRT, **277**, 107949 (2022). DOI: 10.1016/j.jqsrt.2021.107949
[24] A.D. Sappey, R.A. Copeland. J. Mol. Spectrosc., **143** (1), 160–168 (1990). DOI: 10.1016/0022-2852(90)90267-T
[25] R.A. Copeland, B.R. Chalamala, J.A. Coxon. J. Mol. Spectrosc., **161** (1), 243–252 (1993). DOI: 10.1006/jmsp.1993.1229
[26] P.F. Bernath, R. Colin. J. Mol. Spectrosc., **257** (1), 20 (2009). DOI: 10.1016/j.jms.2009.06.003
[27] E.S. Hwang, J.B. Lipson, R.W. Field, J.A. Dodd. J. Phys. Chem. A, **105** (25), 6030 (2001). DOI: 10.1021/jp010088i
[28] A.E. Douglas. Can. J. Phys., **52** (4), 318 (1974). DOI: 10.1139/p74-044
[29] K.P. Huber, F. Holland, J.A. Coxon. J. Chem. Phys., **96** (2), 1005 (1992). DOI: 10.1063/1.462187
[30] Y. Chang, Y. Yu, H. Wang, X. Hu, Q. Li, J. Yang, S. Su, Z. He, Z. Chen, L. Che, X. Wang, W. Zhang, G. Wu, D. Xie, M.N.R. Ashfold, K. Yuan, X. Yang. Nature Commun., **10** (1), 1 (2019). DOI: 10.1038/s41467-019-09176-z
[31] S.V. Kozlov, E.A. Pazyuk, A.V. Stolyarov. Opt. Spectrosc., **125** (10), 445 (2018). DOI: 10.1134/S0030400X18100119.
[32] H.-J. Werner, P.J. Knowles, R. Lindh, F.R. Manby, M. Schutz, P. Celani, T. Korona, G. Rauhut, R. D. Amos, A. Bernhardsson, A. Berning, D.L. Cooper, M.J.O. Deegan, A.J. Dobbyn, F. Eckert, C. Hampel, G. Hetzer, A.W. Lloyd, S.J. McNicholas, W. Meyer, M.E. Mura, A. Nicklass, P. Palmieri, U. Schumann, H. Stoll, A.J. Stone, R. Tarroni, T. Thosteinsson. MOLPRO, Version 2010.1, a package of *ab initio* programs [Electronic resource]. URL: https://www.molpro.net.
[33] Y.G. Borkov, O.N. Sulakshina, S.V. Kozlov, T.I. Velichko. Opt. Spectrosc., **128** (12), 1789 (2020). DOI: 10.1134/S0030400X20120887.
[34] *NIST Handbook of Basic Atomic Spectroscopic Data* [Electronic resource]. URL: https://www.nist.gov/pml/handbook-basic-atomic-spectroscopic-data
[35] S.R. Langhoff, M.L. Sink, R.H. Pritchard, C.W. Kern. J. Mol. Spectrosc., **96** (1), 200 (1982). DOI: 10.1016/0022-2852(82)90226-0
[36] H. Lefebvre-Brion, R.W. Field. *The Spectra and Dynamics of Diatomic Molecules: Revised and Enlarged Edition* (Elsevier Academic Press, Amsterdam, 2004).
[37] G. Li, J.J. Harrison, R.S. Ram, C.M. Western, P.F. Bernath. JQSRT, **113** (1), 67 (2012). DOI: 10.1016/j.jqsrt.2011.09.010